Analytica Chimica Acta 1395 (2026) 345217

Contents lists available at ScienceDirect

Analytica Chimica Acta

journal homepage: www.elsevier.com/locate/aca

Measuring absolute gas amounts with gas chromatography by using a novel setup for pressure based gas control

Andreas Hofmann *, Ingo Reuter, Freya Müller, Anna Smith

Institute for Applied Materials (IAM), Karlsruhe Institute of Technology (KIT), Hermann-von-Helmholtz-Platz 1, 76344 Eggenstein-Leopoldshafen, Germany

HIGHLIGHTS

- Novel gas injection system for gas chromatography and related gas applications.
- Pressure-dependent multi-point calibration with a reference gas system operating under reduced pressure.
- Absolute gas quantification using a built-in loop device.

GRAPHICAL ABSTRACT

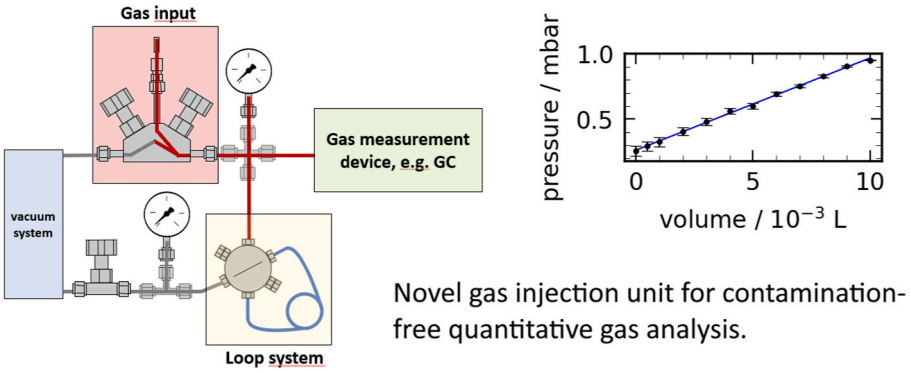

ARTICLE INFO

Keywords:
Gas chromatography
Absolute gas amounts
Quantification
Reduced pressure

ABSTRACT

The characteristics of the gas itself, such as its volatility, compressibility, or weight, often complicate the process of feeding gas into a measuring system, such as a gas chromatograph. This is particularly relevant when quantifying individual gas components. While it is possible to inject gas with syringes, this method has several disadvantages, such as gas tightness and syringe and gas volume, especially for small gas quantities. Therefore, there is an urgent need for a simple, reliable, and improved method of gas injection into a measuring device. This study describes the development of a novel gas injection system that reliably and contaminant-free injects gas into gas chromatography (GC) instruments and other gas-related devices. The system consists of an injection unit, a vacuum system, and a loop assembly, and it connects directly to the corresponding device. Sample gas can then be introduced directly into the evacuated injection system and delivered to the measuring device. The system has been validated using a range of configurations and has undergone extensive testing. Additionally, two applications are presented to demonstrate the system's wide range of potential uses. Notably, the setup enables a contamination-free gas supply from battery pouch-bag cells. For this configuration, an adapter assembly was required for the pouch-bag cell and was integrated into the battery cell. Additionally, it is demonstrated how the setup can be used to determine the gas composition of a thermal decomposition reaction. This setup is a new, platform-independent option for introducing gas into a low-pressure environment and connecting it to devices without causing contamination. Reduced pressure enables multi-point calibration with a single reference or calibration gas mixture, which is pressure-dependent. Additionally, the integrated loop technology allows for the

* Corresponding author.
E-mail addresses: andreas.hofmann2@kit.edu (A. Hofmann), anna.smith@kit.edu (A. Smith).

https://doi.org/10.1016/j.aca.2026.345217
Received 5 November 2025; Received in revised form 16 January 2026; Accepted 7 February 2026
Available online 10 February 2026

quantitative calculation of gas concentrations. Errors in calculating the amount of substance are less than 10–20%, even with flexible pouch cells.

1. Introduction

Gases play a crucial role in many processes and reactions. However, handling them is often more complex than handling solids or liquids. One major challenge is transporting the gas from the sample or reaction site to the analysis tool without contamination, loss, or chemical conversion. When absolute quantitative measurements are required, additional issues arise, such as calibration and determining the total gas amount. Nevertheless, numerous methods and analytical devices are available for gas analysis and quantification. One widely used technique is gas chromatography, which, when combined with suitable detectors, provides high sensitivity and accuracy for identifying and quantifying gases. Gas processes are particularly important in chemical energy storage systems, including secondary batteries based on lithium-ion or post-lithium-ion technologies. After assembling a Li-ion cell, gas evolution can occur under various conditions, such as during cell formation, normal operation, or abuse scenarios.

Moreover, gassing of an operating cell is an indicator for electrolyte decomposition under safety relevant conditions such as overcharge possibly leading to the thermal runaway [1]. For this reason, early attempts were made to elucidate an understanding of gas formation in the case of lithium-ion cells [2,3]. This includes both, the precise determination of the amount of gas formed in a lithium-ion cell as well as the quantitative analysis of the individual gases formed using sophisticated analytical techniques [3–5]. Due to the analytical methods, which often only provide the analysis of certain gases or reaction products, coupling of methods or use of several methods at the same time are also widely applied in order to obtain a more complete picture of the gases formed. This includes e.g. the coupling of gas chromatography (GC) with Fourier transform infrared spectroscopy (FT-IR) [6–8], FT-IR with special gas analyzers [9], FT-IR with μGC [10] or FT-IR with Non-Dispersive InfraRed (NDIR) and paramagnetic analyzers [11].

The GC-MS technique, which is ideally suited for volatile organic solvents, is often limited for gas measurements for several reasons: First, separation of gases requires special columns, leading to sophisticated column setups. Second, higher-boiling volatile organic compounds often cannot pass through the appropriate columns for gas separation and are therefore not detected. Third, the detection of gases by mass (e.g., $m/z =$ 28 for N_2/CO_2) is often difficult. Fourth, each individual gas requires individual calibration; comparison of gases to each other is not possible due to differences in ionization. Fifth, typical single-quadrupole MS instruments are linear only over a small concentration range. This also applies to investigations by means of pyro-GCMS, which are often used to investigate materials and selected components from Li-ion cells (e.g., separators and electrodes) during thermal treatment [12–15]. For this reason, GC-MS analysis is often combined with a more suitable technique or detector for gases (e.g., GC-TCD, FT-IR, gas sensors, etc.).

Naturally, there is a strong interest in detecting the relevant gas species directly during cycling, which is why on-line methods have been developed to allow *in-situ* determination [16–24]. Today, the typical cells used for in-situ gas analysis, namely differential electrochemical mass spectrometry (DEMS) and/or online electrochemical mass spectrometry (OEMS), are specially designed cells, but they are not directly comparable to the typically used commercial lithium-ion pouch-bag, prismatic or round cells due to the necessity of the sophisticated gas adaption, and are not intended for studying longer cell cycling (some hundred cycles) under real conditions. Some cells for DEMS/OEMS analyses can even be purchased commercially (e.g. ECC-DEMS cell from EL-Cell). However, continuous measurements also raise the difficulty of reliably retaining the electrolyte in its original composition despite some attempts are made to overcome this drawback [19]. At the same time, online measurements continuously remove any gaseous products that might further interact as a key component in the cell, so called cross-talk, falsifying real circumstances within the battery cell and hamper effects in the cells caused by the gases. Additionally, continuous gas flow and pressure drops by interrupted gas flow switch is difficult to control and do not reflect the situation in the real cell [24]. Gases that are often described in the context of DEMS and OEMS include hydrogen (H_2), carbon monoxide (CO), carbon dioxide (CO_2), ethane, and ethylene. MS methods are often used in the studies to analyze the gases. However, there are difficulties in reliably identifying and quantifying a single gas species in a mixture of several gases, since identical mass fragments may well originate from different gases (see above). An overview of typically used in situ/operando techniques is summarized in Refs. [25,26], whereas the advantages of individual techniques are presented in Ref. [27]. Although the methodology provides a high benefit in terms of mechanistic studies and fundamental investigations, neither a comparison with commercial cells, nor a direct support for prolonged cycling is possible due to the aforementioned reasons.

For gas volume determination in pouch-bag cells, two methods are commonly used in literature: (1) determination by air/water/oil displacement [2,28,29] and (2) determination by the well-known Archimedes' principle [8,29–33]. Both techniques require the construction of appropriate instrumentation systems but are in principle suitable for gas determinations during operation as well as at the end of cycling and provide information about the total amount of gas that is generated or has been generated in a cell. However, they cannot provide information about the identity of individual gas species. Additionally, it should be noted that the gas amount may be falsified by gas insertion into the porous electrodes [34]. A third possibility, the direct measurement of cell dimensions to estimate gas formation, as also practiced, is subject to relatively high uncertainty [4,35].

There are numerous procedures described in the literature for bringing the evolved gases from the sample/battery cell into the analytical instrument. However, there are no established methods for extracting liquid and solid components from the cell. [36], gas extraction is challenging by the facts that the cell is often still under negative pressure relative to the surrounding atmosphere despite gas formation (exception: gases evolved during abuse scenarios like overcharge, deep discharge or thermal runaway) and that the handling of gases is laborious. Principally, all of the extraction methods can be divided into two main approaches: (1) directly connecting the gas stream to the gas analysis setup device (e.g. by capillaries) including auxiliary assemblies, which then collect the gas from the cell and also forward it directly to the analysis device) and (2) transporting the gas from the sample (e.g., pouch-bag cell or gas sampling box) to the instrument using a gas container (e.g., gastight syringe or a headspace vial). Table 1 provides a detailed list of the different methods described in the literature. However, the exact arrangement of the construction reported often remains unclear, especially how exactly the gas sampling/connection was carried out, so that an assessment to the discussed values/estimation of the accuracy is difficult and the reproducibility of the procedure is not given [6,10,28,37–46]. Furthermore, any source of leak or contamination cannot be reconstructed.

Generally, the existing methods of gas injection into a GC instrument by syringe or headspace vial cause a number of issues and disadvantages.

- An overpressure or normal atmospheric pressure is required to reliably fill the syringe.
- A residual amount of ambient gas usually remains in the needle.

Table 1
Overview about extraction methods and gas sampling for Li-ion batteries and gas chromatography analyses.

Transportation of gas from a sample (e.g., pouch-bag cell or gas sampling box) to the instrument using a gas container (e.g., gas-tight syringe or a headspace vial).	
Gastight syringe, extraction from pouch-bag cell	[7,8,31,33,47–54]
Gastight syringe, extraction from gas sampling box	[55,56]
Gastight syringe, extraction from reaction vessel, Li determination	[57,58]
Gastight syringe, extraction from glass cell	[59]
Gastight syringe, extraction from reactor	[60]
Gastight syringe, extraction from pouch-bag cell opening device	[61–64]
Gastight syringe, extraction from headspace vial or bottle	[65]
Gastight syringe, extraction from adaptor which is built on pouch-bag cell	[29]
Headspace vial, use of Solid Phase Microextraction with gasflow from Li-ion cell	[66,67]
Gas bag, extraction from reaction vessel	[46]
Headspace vial, without cell connection	[65]
Adaption of the gas stream to the analysis system	
Direct adaption (not specified)	[6,44]
Direct adaption, extraction from sampling vial by using liquid nitrogen	[68,69]
Direct adaption by a capillary column	[70]
Direct adaption, valve port approach with flow control	[71]
Direct adaption, Ar line	[45]
Direct adaption, gas flow from an open pouch cell in a steel container	[72]
Direct adaption, via dilutor and pump	[9]

- Even when using a septum, there is always a risk of puncturing the sample and contaminating it with the outside atmosphere.
- If septa are applied to the samples (fixed with adhesive tape or bonded with sealant), there is a risk of the sample being contaminated by these materials or adhesives.
- To determine absolute quantities, the total amount of gas must be known. This requires additional measurements.
- High-precision, gastight syringes are expensive and require extensive cleaning.
- Reliable calibration requires several calibration mixtures with different concentrations.
- Gas sampling always damages the outer membrane/layer of the sample, rendering it no longer hermetically sealed. Further use of the sample (e.g., pouch bag cells) under defined conditions (e.g., water content) is no longer possible.
- To achieve balanced pressure, extra gas is often added, which dilutes the sample (e.g., Ar, N_2) and complicates analysis: First, exact amounts of the diluent must be accounted for. Second, if gases are diluted below the detection limit, analysis becomes more challenging.
- When using small amounts of gas (e.g., 5–100 μL), the error ranges are large due to pressure fluctuations.
- Headspace and solid phase microextraction (SPME) approaches are to a large extent dependent on the particular analyte and sample matrix. However, the exact composition of new samples is often not known.
- Glass surfaces in headspace vials can react with cell gases (e.g. HF, PF_3, etc.) and cause additional signals.
- Quantification with headspace technique is time-consuming and requires a high level of understanding.

On the other hand, there are also major challenges for the direct adaptation systems that exist so far.

- Very specialized equipment or setups are needed, which involve sophisticated circuits and require a high level of user expertise.
- The conditions within specially designed cells are often not directly comparable with commercial cells.
- Dilution of the sample is often necessary due to the use of large containers (≥100 ml, often under pressure).
- Quantitative measurements are costly and also require the use of several expensive calibration gas mixtures, especially when used with GCMS due to its non-linearity.
- Adaptation to other sample containers is not easily feasible due to special designed setups (often hand-made connection).

For this reason, there is a great request for a simple but reliable system that addresses and solves these issues.

Consequently, this study will implement a novel gas application technology that facilitates reliable identification of the gas composition through the use of reduced pressure and a direct connection to the analytical device. Based on these measurements, the gas volume can be determined through calibration, and then the absolute volume of each gas can be calculated, including the absolute amount of substance. The goal is to enable the determination and quantification of the gases formed in the bag cell at low or reduced pressure without adding additional gas.

2. Materials and methods

2.1. Chemicals and materials

A gas mixture (Basi Gas) composed of acetylene, hydrogen, ethylene, methane, nitrogen, carbon dioxide, carbon monoxide and helium in argon was used for the gas calibration (see Table SI–1 in the supporting information for precise composition). The gas was chosen because it includes most of the gases found in the battery field and is easily accessible. This gas was stored and handled in a cold place. Depending on the concentration of CO, it is essential to use a CO monitor in the laboratory for safety reasons! If other toxic gases are used, additional safety precautions may be necessary, depending on the gas used. Selected volumes were taken up with a gas-tight syringe and inserted into the novel gas adaption system. For the pouch-bag cells, NMC cathode material, ceramic coated separator, graphite anode material as well as electrolyte (EC:DMC 1:1 vol.-%, 1 M $LiPF_6$, 3% VC) was used. Lithium oxalate was purchased from Sigma-Aldrich and used without purification.

2.2. Cell assembly

Cell assembly of the pouch-bag cells was done on a semi-automated manufacturing line within KIT-Battery Technology Center, as published in Ref. [73]. Details are provided in the supporting information (section 3). Typically, the pouch bag cells are sealed under reduced pressure automatically at ~30 mbar.

2.3. Gas chromatography

Gas chromatography experiments were performed on a Clarus 690 GC from PerkinElmer Inc. (Waltham, USA) equipped with an Arnel system 4019, and two thermal conductivity detectors (TCDs) and a MS detector (SQ 8S). The software packages used for data acquisition were TotalChrom 6.3.4 (samples of the gas mixture) and Turbomass 6.1.2 (samples with electrolyte vapor). For data analysis of the TCD data the TotalChrom 6.3.4 package was used. The carrier gases were He 6.0 (99.999%, Air Liquide) and N_2 (99.9999 %, Air Liquide). (Nitrogen was carrier gas for the detection of helium and hydrogen.) The 624 GC column (Elite, PerkinElmer Inc.) with a length of 60 m and an inner diameter of 0.25 mm and a fim thickness of 1.4 μm was used for GC-MS measurements. For the data acquisition, three different detectors were used (TCD-1, TCD-2 and MS). Both TCDs were heated to 100 °C with a range of 3 and an attenuation of −1. Due to the set-up of the GC Arnel device with some columns relevant for the gas analysis in the GC oven, the detection with the TCDs in the Arnel system had to be completed

before the GC column gradient (for MS analysis) was started. The columns of the Arnel system were tempered at 92 °C for TCD-1 and at 40 °C for the TCD-2. The GC oven program started with holding the temperature 24 min constant at 40 °C before starting the gradient with a heating rate of 30 °C/min until 230 °C and holding the temperature constant for 29.67 min. The detection with the MS took place in scan mode. A range from 18 u to 250 u was scanned with a scan time of 0.3 s and an inter-scan delay of 0.02 s.

2.4. Gas inlet setup

All components of the assembly (valves, diaphragm valves, flow regulators; see below, Figs. 2–4) were assembled in oil-free and grease-free quality by Swagelok. The pipes are specially cleaned 1/16″, 1/8″ or 1/4″ stainless steel. A brass pipe was used to connect the vacuum and nitrogen line. For more precise determination, the manometers M1 and M3 (see Figs. 2 and 3) were realized as digital manometers (reading accuracy: 1 mbar and accuracy of <0.25% full scale output, PCE, PCE-DPG 3). In case of manometer M2, a high precision digital manometer from Wika was used (CPG1500, reading accuracy: 0.1 mbar and accuracy of 0.25% full scale output). The gas volumes were determined by feeding sample gas through either a syringe or a mass flow controller (MFC, Analyt, SRC-SMC01 M, high accuracy) into different switched gas paths and then determining the corresponding volume using the ideal gas equation ($pV = nRT$; n = mol of N_2 injected and p = pressure difference before and after injection, V = volume, T = temperature, R = universal gas constant). N_2 gas was used because Ar gas resulted in problems in case of some manometers. Since evacuated gas pipes are used and gas can be introduced under pressure, care must be taken to ensure that the screw connections are secure and, if necessary, that splinter protection is provided. Between individual measurements, it is important to allow the system sufficient time to relax completely. To this end, it is extremely important that the system is completely sealed and that there are no leaks anywhere. Typically, we waited at least 1.5 min after introducing the gas before taking a stable pressure measurement. It should be noted that the large number of connection points represents a high risk for leaks. While these were retained in the study due to their flexibility, it makes sense to switch to permanently connected lines when setting up a long-term system.

2.5. Sample Preparation

In the study, different kinds of sample extraction methods were investigated and used.

For a direct injection with gas from gas-tight syringes, a 1/8″ Swagelok adapter with a septum inside was attached on the gas line (1/16″) into the GC device. By using Luer lock one-way adapters (Art.: Braun™ 4099117) for closing the gas volume in the syringe common plastic syringes were used which facilitate the use and cost significantly. The pouch bags with a Swagelok quick connect adaption tool (see below, Fig. 9) were directly interfaced with the new GC inlet setup under reduced pressure in order to extract the gas inside of the pouch-bag cell. The Swagelok connector (male/female quick connect) has been selected to be closed in both directions when disconnected and open in both directions when connected and joined.

For gas calibration, a well-defined amount of calibration gas (1 - 10 mL) was taken with a syringe from the calibration gas bottle and injected either directly into the Arnel gas line followed by an expansion to normal pressure, or into the newly developed gas interface which was also equipped with a septum. The test system was directly connected to the MFC in order to be able to inject nitrogen in a controlled and contamination-free manner.

2.6. Statistical methods

As described in the text, volume and pressure measurements were performed several times and then the corresponding mean values with the respective errors (standard deviations) were specified or shown in the figures. Unless otherwise stated, three individual values were used in each case.

3. Result and discussion

3.1. GC setup

A Clarus 690 Arnel 4019 standard gas chromatograph (GC) from PerkinElmer was used for the investigation and study. In addition to gas determination by means of thermal conductivity detectors (TCD), which are able to detect a gas species starting from ~100 ppm in a gas sample, the instrument is also equipped with a mass spectrometer (MS) for detecting components containing more than two carbon atoms. In this way, the instrument can be used to analyze gases via the TCD detectors (H_2, He, CO, CO_2, CH_4, Ar, O_2, N_2, C_2H_4, C_2H_4, C_2H_6) and gases starting from C_3 via the MS detector. The measurement of highly reactive gases (e.g. HF) is not possible with GC methods due to reactions with the packing material contained in the separation columns. The gas is added via sample loops connected by an onboard gas delivery system. Starting from the gas inlet (inlet), the introduced gas is passed continuously through a sample loop system (sample loop 1 - 4) with defined sample volumes (see Fig. 1). These are then switched in a time-controlled manner after starting the measurement, and the gas is introduced into the corresponding columns. With the columns described above, it is possible to detect, separate and quantify the compounds mentioned above. The advantage is that the gas components have defined retention times due to the GC design. In addition, the last loop switches into the mass spectrometer, allowing either a confirmation of the gas composition or a detection of additional gases and volatile compounds, depending on the column used. Despite the initial contradiction, gas injection via sample loops as shown in Fig. 1 is a prevalent commercial practice, and devices configured for this method are readily available for purchase.

Due to the difficulty of quantifying partially vaporized components in a meaningful way, the MS is mainly used for the analysis of gases (instead of quantification). All loops are inhoused in a temperature-controlled box in order to prevent gaseous products from condensation. Overall, the setup allows for the measurement of the different components in a single sample run, so that a complete analysis is possible with a single gas injection. The setup requires the over-purge of the gas volume for the purpose of eliminating air in the gas system under normal conditions of use. In addition, the measurement of small amounts of O_2 and N_2 is subject to some error. With calibration including several different gas concentrations (calibration gas mixtures) it is possible to obtain relative gas amounts in an unknown gas sample (ppm content). Furthermore, to determine absolute amounts of gas generated in a sample (e.g. battery cell), either an internal standard or knowledge of the total amount of gas generated (gas volume in total) is required.

3.2. Gas inlet setups

Four different sample loading configurations are presented below and used in the manuscript, namely the *standard setup with septum* (SSS), the *gas inlet setup 1* (GIS1), the *gas inlet setup 2* (GIS2) and the *simplified test system* (STS). All systems are specified in detail in the following description and differ on complexity and features.

3.2.1. Standard setup with septum (SSS)

The SSS is typically used to inject the sample into the GC loop system. It consists of a gas line on the GC side that is closed by a septum on the inlet side. The outlet side of the GC, on the other hand, is open to the atmosphere. The sample is injected through the septum with a syringe, flushed through the GC device, and exits via the outlet. Extensive

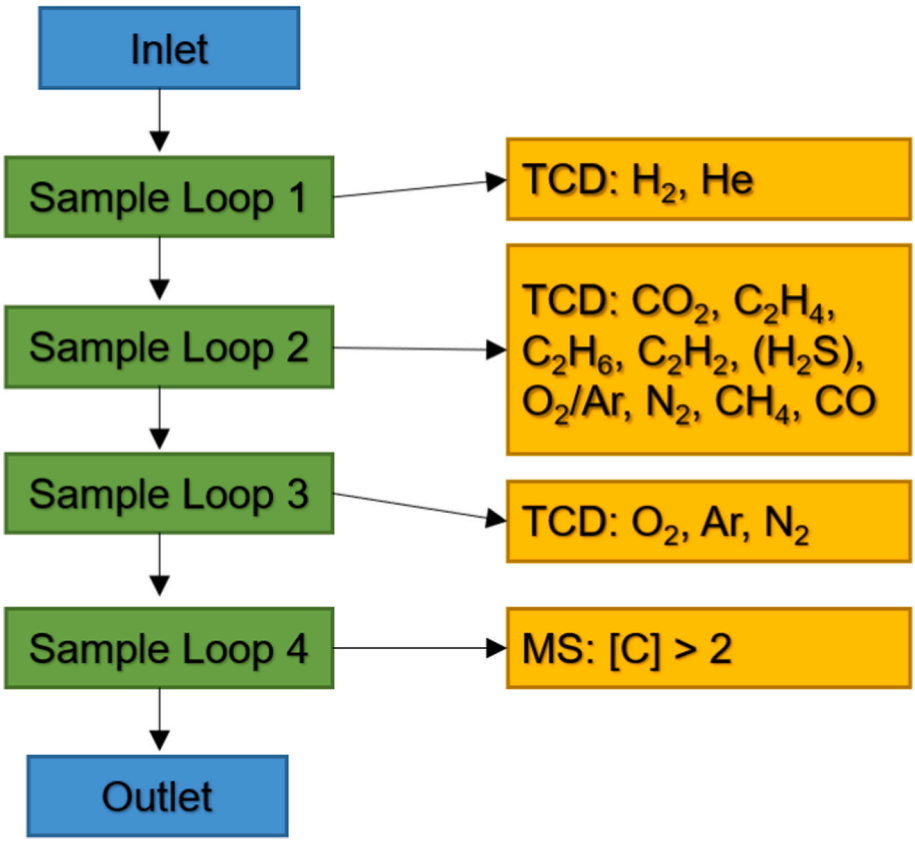

Fig. 1. Schematic illustration of the loop system of the GC device used in the study including the compounds which can be determined with the selected loop control.

flushing with the sample ensures the gas line is completely filled with sample gas. In principle, gas under overpressure conditions (e.g., a pressurized sample bag) can be purged into this setup by expanding it against atmospheric pressure. However, several drawbacks arise when using this setup, including issues with gas transfer from pouch-bag cells or other gas bags.

- Calibration requires the use of calibration gas of various concentrations. This necessitates the use of several expensive calibration gas mixtures.
- The sample gas chamber must be purged several times to displace the air or previous gas samples, so a relatively large sample gas volume is required.
- Samples with low-boiling components can contaminate the gas paths and must be flushed out in an extensive manner.
- For the determination of absolute quantities either an internal standard or the exact knowledge of the gas volume of the sample is necessary. However, both quantities are rather difficult to determine and contain a high uncertainty factor, and furthermore, they are difficult to adapt directly in a battery cell.
- It is mandatory to have an overpressure in the sample to be able to introduce enough gas into the instrument. Often, however, only a small amount of gas is generated in batteries during formation or normal use.
- The use of a gas-tight syringe is prone to errors.
- A measurement to determine the background signal is not possible after the syringe is connected (except when using very expensive special syringes with a valve) since the gas is only displaced.
- The handling with adhesive tape on pouch-bag cells (to use syringes to extract gas from the cell) is not well-established due to the potential of contamination of the electrolyte with the glue or dissolution of polymer components.
- Pouch-bag cells must be pierced and can therefore no longer be cycled under fully closed conditions even with a septum. Additionally, adhesive might contaminate the electrolyte.

3.2.2. Gas inlet system without pressure assistant volume determination (gas inlet setup 1, GIS1)

To overcome some of the main issues of the simple standard setup with a septum (3.3.1), we designed a special inlet approach called GIS1 with an adjustable vacuum and controlled sample loading option, which includes the following three individual parts: (a) “vacuum system”, (b) “inlet system” and (c) “outlet system”, all shown in Fig. 2.

The first part of the GIS1 (vacuum system) consists of the source of inert carrier gas (e.g. Ar or N_2) and the vacuum system. The flow of the inert gas is controlled by an oil-free and grease-free needle valve (B1) and a diaphragm valve (A1). Similarly, the vacuum is adjusted by a second set of these types of valves (B2 and A2). The second part of the system (inlet system) consists of the sample feed. A multi-valve manifold is used for this purpose, and its flow is controlled by two diaphragm valves (A3 and A4). The sample injection is realized through a Swagelok quick coupling system, where half of the quick coupling is permanently installed on the setup, while the other half can be variably connected to various kinds of adapter systems. In the simplest case, this is again a septum that has been inserted into a Swagelok fitting (Fig. 2, part D). Between the second (inlet system) and third sections (outlet system), there is the sample loop system of the GC instrument. The third section allows the entire gas input system, including the sample loops, to be placed under vacuum to remove sample residue or atmospheric gases from them. It consists of a needle valve (B3) and a diaphragm valve (A5). In case of vacuum, the diaphragm valves A1 and A5 must be closed to allow vacuum on all loops. The pressure in the system is monitored by two pressure gauges. One manometer (M1) is located between the two needle valves that control the pressure upstream of the inlet system. The other manometer (M2) is located in the third part of the assembly and

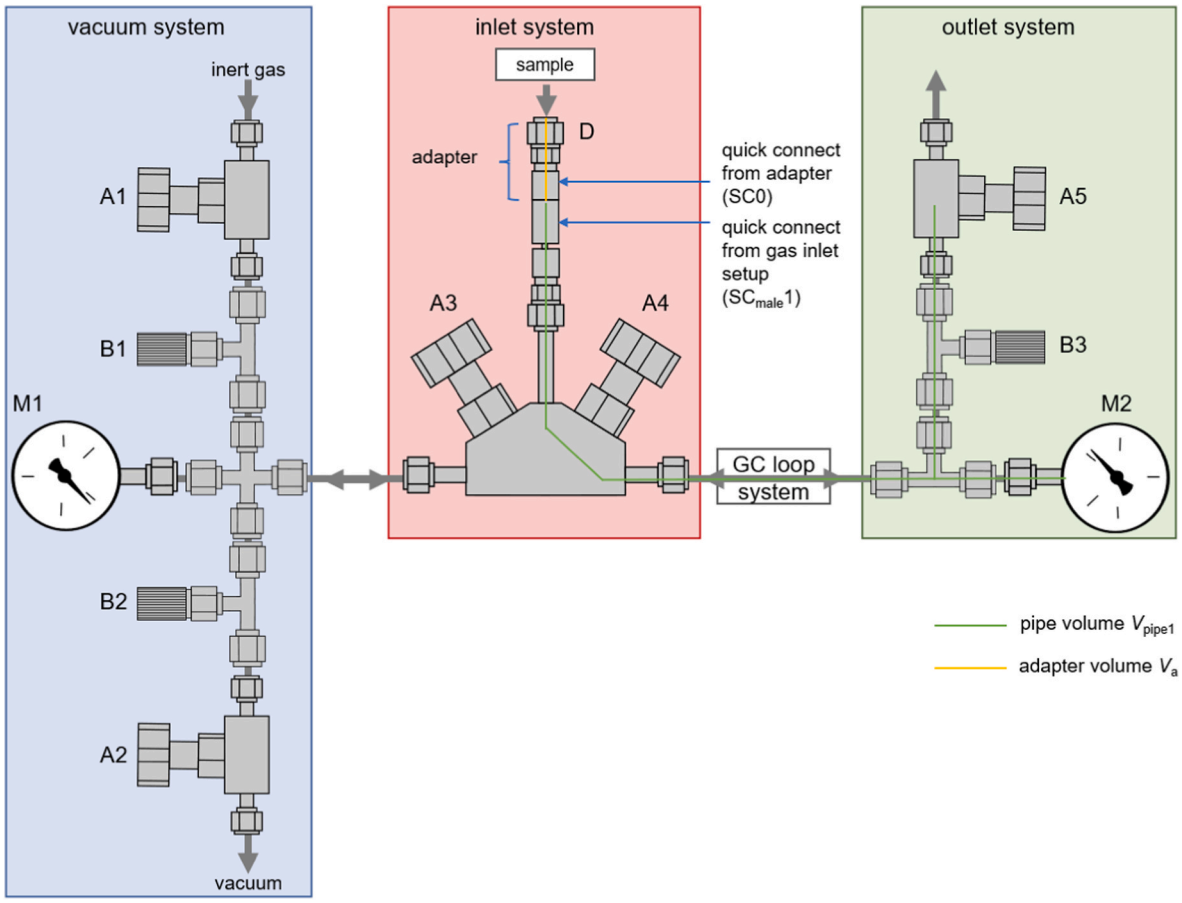

Fig. 2. Scheme of the novel "gas inlet setup 1" including "vacuum system", "inlet system" and "outlet system". A = diaphragm valve, B = needle valve, D = Swagelok fitting, M = manometer, GC = gas chromatography device.

monitors the pressure during injection. The setup can be used under reduced pressure (small sample volume and injection into an evacuated system) as well as under normal pressure (large volume samples) or, in the simplest case, analogous to the *standard setup with septum* by flushing the sampling gas through it.

Such a device makes it possible to avoid and eliminate some of the main disadvantages of the "standard setup" described in 3.3.1, namely.

- Low-boiling compounds from battery electrolytes (e.g. dimethyl carbonate) can be more readily removed under reduced pressure (prevention of contamination).
- Calibration is possible under reduced pressure conditions. Then only one calibration mixture is necessary for creating a pressure dependent calibration curve. This requires that the sample volume is limited to the evacuated volume or only little more (measurement in small overpressure condition is possible).
- The amount of sample and/or calibration gas, which is required for measurements, is significantly lower than for purging operations because removal of air/previous gas samples or residues by flushing of the pipes is no longer necessary.
- The setup can be used in a simple manner to connect other gas devices (see below).

Nevertheless, some drawbacks remain, especially when using a septum for the gas inlet (filling of sample gas by syringe) and a normal pouch-bag cell without additional adapters. These drawbacks are summarized in sections "quantification" and "gas transfer" (see 3.3.1 and introduction, respectively).

The setup can be used in an excellent and reliable manner to determine gas volumes that are known, i.e. when a syringe is completely emptied after gas injection, or when a known amount of gas is introduced into the system. If these requirements cannot be met, e.g. when connecting a pouch-bag cell, gas bag or a gas container with an unknown gas volume/pressure, or when only part of the sample gas is introduced to the inlet system, the setup does not allow to calculate absolute gas amount of a gaseous species which are present in the sample gas. In this case, the addition of an internal standard or the exact knowledge of the gas volume in the part to be connected including the piping is necessary. Although there are possibilities to add internal gases before gas measurement or to determine the gas volume (e.g. Archimedes approach), both of them are difficult to realize and involve errors (see also section 3.3.1). In this respect, there is further interest to adapt the setup for enabling sample measurements in such cases.

3.2.3. Gas inlet system including pressure assistant volume determination (gas inlet setup 2, GIS2)

To further improve the inlet device, an advanced pressure/volume determination unit was developed and added ("volume control" unit) in order to allow the quantification of gas volumes more precisely, shown in Fig. 3. The whole setup including the "volume control" unit is called GIS2 (Fig. 3). In principle, the setup works analogous to GIS1, but with the option to additionally determine the total gas volume and the internal pressure of the sample container. However, this is limited to the condition that samples used, are non-compressible.

If the valve (in the simplest case a 6-port 2-position valve with manual control) of the "volume control" system is switched to off, there is initially vacuum on the sample loop of the "volume control" system and vacuum on the setup ("inlet system" and "outlet system"). Both enlarged caps of the 6-port valve (volume control) indicate that they are closed to the outside (blind plugs). The two valves to the right with the

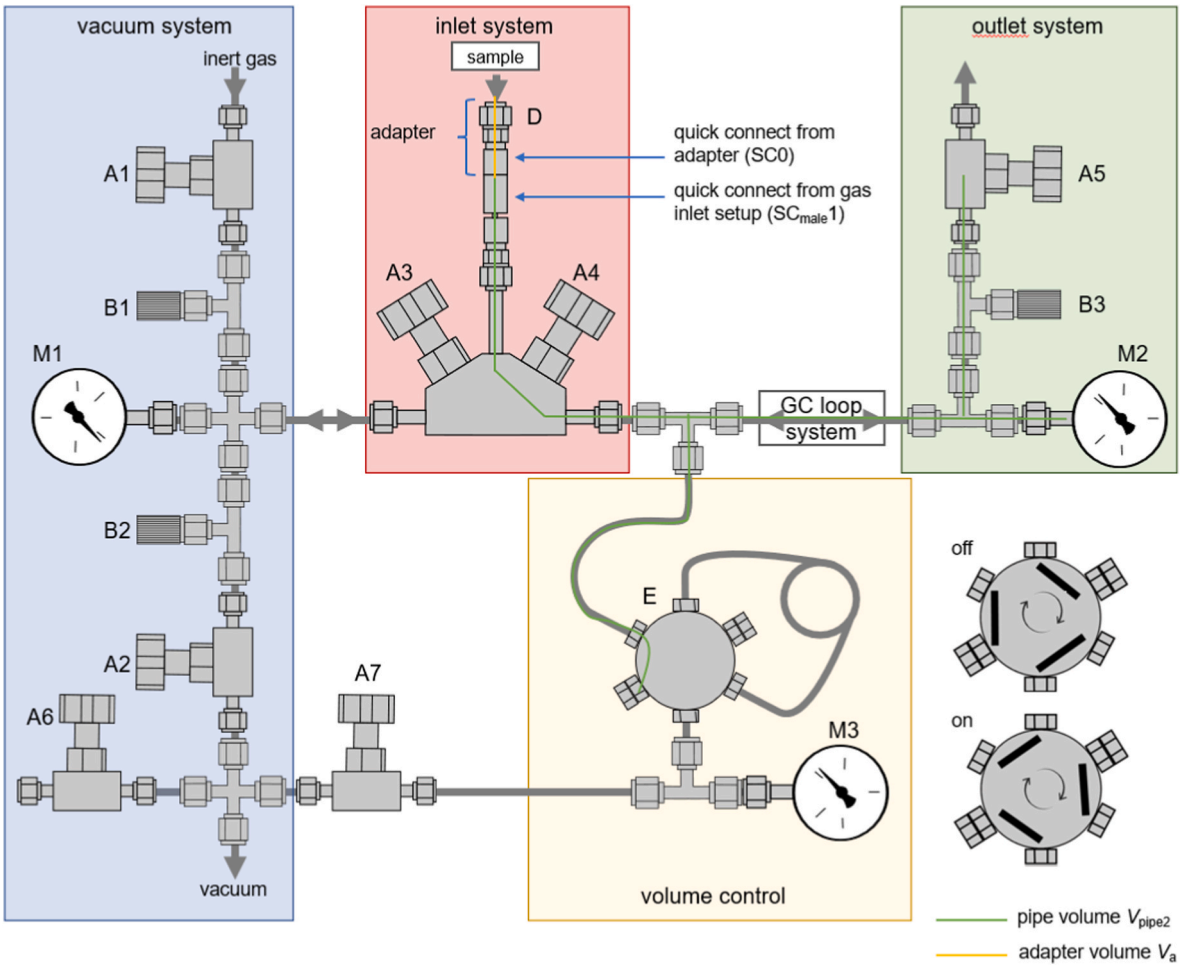

Fig. 3. Scheme of the "GC inlet setup 2" including "vacuum system", "inlet system", "outlet system" and "volume control". A = diaphragm valve, B = needle valve, D = Swagelok fitting, E = 6-port-2-position valve, M = manometer, GC = gas chromatography device.

black bars indicate the flow paths in the corresponding state "on" vs. "off". The pressures can be read directly from the two manometers M2 and M3 and should be equal in the evacuated state. The measurement of the fully evacuated system can now be carried out by first closing the vacuum on the "inlet system" (A3 closed) and connecting the sample with an unknown gas quantity (with constant volume) to the sample port D. For that purpose, a Swagelok quick connect male adapter is located on the gas inlet setup device. This adapter is closed to atmosphere when disconnected and open when connected to a corresponding female quick connect counterpart located at the sample. With gas insertion, the pipe on the system side is filled with gas from the sample. This can be controlled by checking the resulting pressure on the manometer M2. Subsequently, the pressure is read at M3 and the valve in the volume control is switched to on, so that a part of the system pressure is purged into the vacuumed loop with known volume. Subsequently, the pressure change of M2 is noted again. The GC measurement can then be carried out. Please note that valve A6 was introduced to allow for direct linkage to a vacuum, e.g., for a sample bag or evacuation of the gas filling system (see below).

3.2.4. Simplified test system (STS) to evaluate gas inlet setup 2

In order to accurately verify the GIS2, the GC line was blocked and an additional highly sensitive pressure gauge (M2) was integrated (Fig. 4a). This setup is referred to as the STS in the following. Additionally, a *gas filling system* was developed to fill the sample containers (rigid steel container or elastic cell) with gas very precisely (Fig. 4b).

Miniature Swagelok couplings were used to connect the sample containers to the STS and evacuate the gas filling system. This is done through the $SC_{female}2$ and $SC_{male}1$ positions and the corresponding connections are precisely labeled in Fig. 4. For setting up a defined gas volume, a mass flow controller (MFC, valve on exit-side to enable reduced pressure) was used. Nitrogen gas was used as a test gas to evaluate the system.

Since the Swagelok quick connect system releases a small amount of gas (air) into an evacuated system when it is joined together, some air is flushed into the gas filling system, when both sides are connected. Therefore, to exclude a change in the gas amount of the sample (V_{cont} or V_{cell}), this sample device was additionally separated by the valve A6. In order to examine both variable and fixed housings, the two sample vessels (rigid steel container and an elastic pouch bag cell) were selected. For clarity, all gas paths and abbreviations are summarized briefly in Table 2 (see also supporting information, Table SI–2).

3.3. Gas injection by using a syringe under normal pressure (1atm) compared to gas injection into an evacuated pipe system

A comparison between two different gas sampling methods, namely gas injection via syringe under normal pressure (in other words, after the gas is fed, it expands against the normal atmosphere) and gas injection via syringe into an evacuated pipe system, was done with known calibration gas mixtures (Fig. 5). Indeed, the standard setup with septum (gas sampling under normal pressure) as well as the gas inlet setup 1 (gas sampling into an evacuated pipe system) approach were used for the comparison. Since both setups, namely GIS1 and GIS2, basically do not

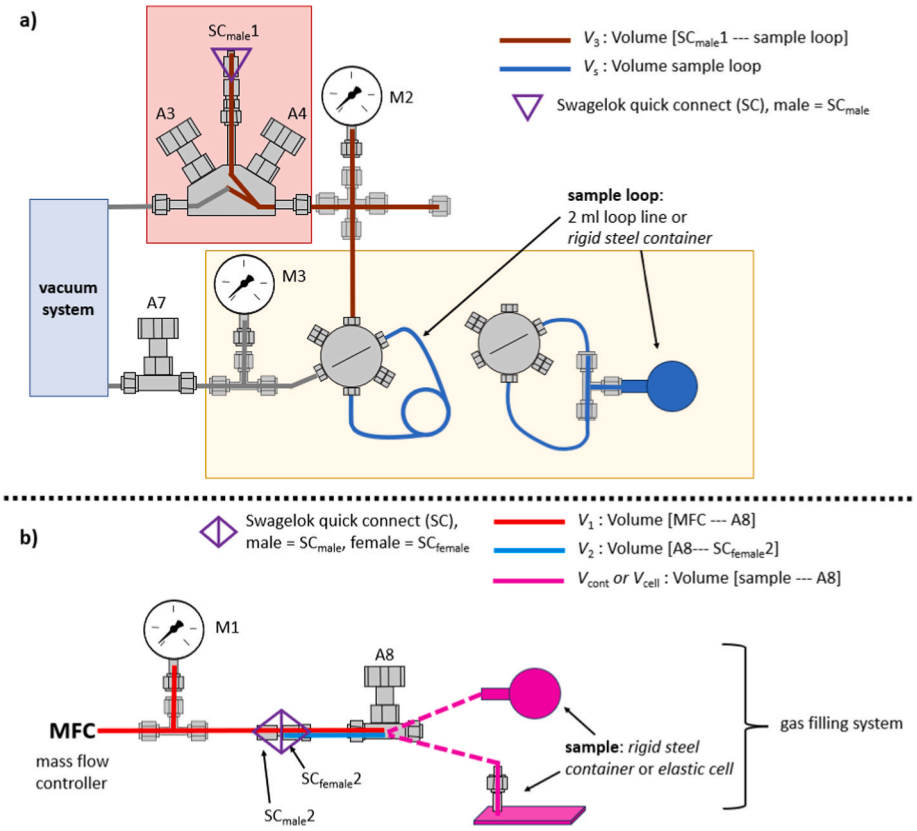

Fig. 4. Simplified test system (a) and gas filling system (b). The different volumes of the pipe systems are shown in different colors. The gas sample can be inserted either via a rigid steel container or an elastic pouch-type bag (without electrodes or electrolyte). A 2 ml sample loop (loop line) or a rigid steel container is used for the sample loop. A = diaphragm valve, M = manometer, SC = Swagelok quick connect. (For interpretation of the references to color in this figure legend, the reader is referred to the Web version of this article.)

differ when used with a syringe (except for the little longer pipe system in GIS2), the comparison here was only performed using the GIS1-setup. For this purpose, selected gas amounts of the calibration gas (0.5 mL - 10 mL) were injected by syringe using a septum closed adapter.

In Fig. 5a, the correlation of the peak area to the injected volume is shown in case of the standard setup configuration (standard setup with septum). It can be observed that the peak area of most of the gases is increasing, until 3 mL of the injection volume is reached. The peak areas remain almost constant above a 3 mL injection volume because the concentration remains constant once the pipeline is filled with gas and the gas expands to the atmosphere. Surprisingly, the minimum amount of 3 mL calibration gas is relatively small compared to the recommendation to flash extensively to ensure a homogeneous gas filling. However, since the relevant gases were introduced with the first two sample loops, the following sample loops including the MS line do not necessarily have to be completely purged with sample gas as well, so measurements performed with sample loops 3 and 4 may still require a higher total sample gas volume. It can be observed that the first sample loop (H_2, He) is obviously already sufficiently filled with 2 mL, while the other gases (sample loop 2) require 3 mL of calibration gas. A systematic calibration with different gas concentrations including the linear fit is shown in the supporting information (Fig. SI–1).

Since in all cases the applied gases were expanded to atmospheric pressure, the observed TCD areas exhibit the same response in all cases. This is in contrast to the novel GIS1-setup (Fig. 5b), where the signal area increases depending on the amount of gas introduced. Depending on the gas sensitivity, different areas with different increasing linear curves are received. Thus, it is seen that the gases exhibit different gradients, with H_2 showing the smallest slope and CO_2 the highest slope. The evolution of the peak areas with the novel GIS1 reveals some differences related to the standard setup. Firstly, the quantification of gases is now possible with a volume of only 0.5 mL of calibration gas (a smaller value might also be sufficient but was not tested here). Secondly, the peak areas do not converge in the tested range but indicate a linear behavior which enables the use of a pressure-dependent calibration with only one calibration mixture. Thirdly, the filling into an evacuated system allows a uniform and homogeneous filling of all sample loops. A deviation from the ideal linear behavior is due to slightly different initial vacuum values and the introduction of the reference gas with a syringe.

The injection of different gas volumes into the GIS1 is depicted in Fig. 6. In this case, particular emphasis was placed on ensuring identical initial conditions (vacuum and syringe filling) to significantly reduce errors. A linear correlation between the pressure and the gas volume can clearly be observed. This allows for the calculation of the injected volume of gas samples based on the pressure detected by the electronic manometer during the sample loop switching. In addition, the correlation between gas volume and pressure allows for the calculation of the total amount of gas injected to get a semi-quantitative information about the analyzed gas, with the condition that less than 10 ml are injected (within the calibration range). Within the study it could be shown that the linear relationship is still maintained even with an increase of the input gas volume (with relative pressure increase into the positive range), so that in principle the possible gas volume can be increased. It should be noted that this only applies in the case of complete gas injection (e.g. using a syringe, etc.). In summary, it can be concluded that the novel technique using reduced pressure represent a significant improvement over the standard procedure (SSS).

Table 2
Abbreviations used in the study for gas volume, pressure and amount of substance. Three consecutive short lines represent the gas line between the two specified terminal connection points.

abbr.	explanation	abbr.	explanation
V_1	volume [MFC — A8]	V_{pipe1}	volume of the pipe in GIS1
V_2	volume [A8 — $SC_{female}2$]	V_{pipe2}	volume of the pipe in GIS2
V_3	volume [$SC_{male}1$ — sample loop input]	V_s	sample volume in general (including syringe)
V_{SL}	volume [sample loop]	p_s	pressure of gas sample in V_s
$V_{SL,cont}$; $V_{SL,loop}$	[sample loop]: steel container or 2 ml sample loop	p_0	pressure before gas supply from MFC in volume [MFC — elastic cell] or [MFC — steel container]
V_{cell}	volume [A8 — elastic cell]	p_1	pressure in volume [MFC — elastic cell] or [MFC — steel container] after gas supply from MFC
V_{cont}	volume [A8 — steel container]	p_2	pressure in volume V^1 before gas is injected
V^0	volume [MFC — gas sample]	p_3	pressure in volume $V^1 + V_{cell}$ or $V^1 + V_{cont}$ after gas is injected
V^0_{p0}	volume [MFC — elastic cell] at p_0	p_4	sample loop pressure before gas injection
V^0_{p1}	volume [MFC — elastic cell] at p_1	p_5	pressure in volume $V^1 + V_{cell} + V_{SL}$ or $V^1 + V_{cont} + V_{SL}$ after gas injection into loop system
V^1	volume [A8 — sample loop input]	n	amount of substance of N_2 from MFC, 1 ml equals $4.1438 \cdot 10^{-5}$ mol
$V_{cell,\ p1}$	volume [A8 — elastic cell] at p_1	n'	remaining gas (amount of substance) of N_2 in V^0_{p0} at p_0
$V_{cell,\ p3}$	volume [A8 — elastic cell] at p_3	n''	remaining gas (amount of substance) of N_2 in V^1 at p_2
$V_{cell,\ p5}$	volume [A8 — elastic cell] at p_5	n'''	remaining gas (amount of substance) of N_2 in V_s at p_4
V_a	volume [D — SC0] (volume of the septum adapter)	n_{cont}; n_{cell}	amount of substance of N_2 in V_{cont}; amount of substance of N_2 in V_{cell}

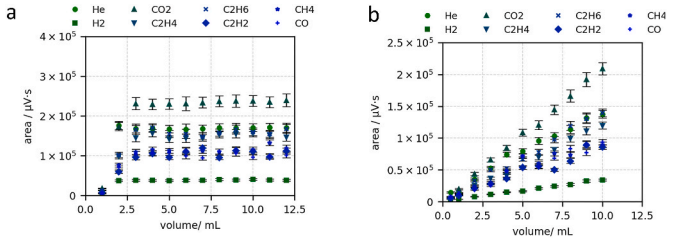

Fig. 5. a shows the peak area of the selected gas species (calibration gas mixture) versus the injection volume with the standard setup. Fig. 5b: Volume-dependent signal peak areas of individual gases (with an identical calibration gas mixture) measured with the "gas inlet setup 1." "Volume" refers to the gas volume injected into "gas inlet setup 1," which was set under vacuum beforehand.

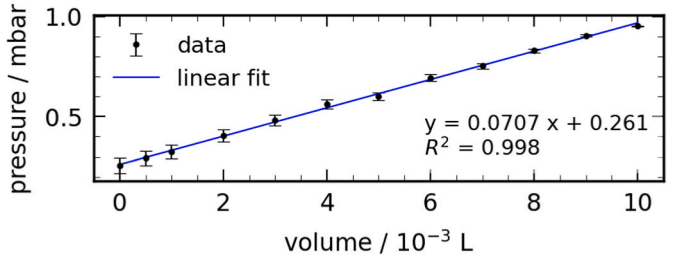

Fig. 6. Pressure dependence (absolute pressure) on change in gas volume by syringe sample insertion in the case of gas inlet setup 1.

3.4. Quantification in case of GIS1 and GIS2

In the simplest case, the setup can be used such that the sample gas is injected at normal pressure and expands against normal pressure (valves in the "outlet system" are open). In this case, the measurement corresponds to a usual injection according to the standard setup with septum at normal pressure. A calculation of the substance quantities is carried out here according to the common methods: calibration with calibration gas mixtures, determination of the signal intensities and recalculation of the obtained signal intensity area (TCD) from the sample gas to concentration and to the substance quantity (via loop volume). As a basis, calibration measurements must therefore be carried out before or directly after the sample measurement in order to determine the intensity of the individual substances at defined gas addition quantities in the TCD detector. If the setup is used to inject the gas into an evacuated system (i.e. the valves in the outlet system are closed), the measurement is basically similar. The calibration gas or sample gas is introduced into the evacuated system via a septum, and the gas is uniformly distributed in the pipe system V_{pipe1} (or V_{pipe2} for GIS2) and the volume of the septum adapter V_a. Peak areas are determined according to the quantity of the individual substances introduced, so that it is then possible to recalculate the absolute quantity in the sample gas according to the peak area. In principle, the total volume can be determined via the pressure increase, provided that the gas is completely introduced into the system but is not known (e.g. via a syringe containing gas from pouch-bag cells). Due to the concentration measurements at different pressures, a multi-point calibration can be performed very easily with a calibration gas mixture. Fig. 7 shows the calibration measurements for the experimental setup with the concentrations of the individual substances in the calibration gas given in the experimental part as a function of the peak area as a function of the amount of substance introduced which are measured with the GIS1 under reduced pressure (injection of the gas volume into an evacuated pipe system).

As mentioned before, the GIS1 can therefore be used for the determination of absolute amounts of substances when the entire gas volume is applied completely to the analysis system. The calculation of the gas amounts is briefly outlined and described below:

Note that ideal gas conditions are assumed at all times. Initially, the entire gas sample volume is located in the gas sample container (e.g. syringe) with volume V_s (syringe volume) and pressure p_s (usually p_s is atmospheric pressure). During sample loading, the whole gas amount is then inserted into the gas pipe system with $V_{pipe1}+V_a$, resulting in a final pressure p_2 in the pipe system. For gas calibration, the amount of substance n_i which is contained in the calibration gas with the mole fraction α, is then obtained according to equation (1).

$$n_i = \alpha\, n_{tot} = \alpha\, \frac{(V_{pipe1} + V_a)p_2}{R\,T} \tag{1}$$

These calculations allow a linear regression to be carried out and consequently the quantification of the amount of gases in real samples without dilution of the sample. The precise data of the fitting results are shown in the supporting information (Table SI–3). The coefficients of determination (COD, R^2 value) range between 0.971 for carbon monoxide and 0.994 for ethane. These values are in good agreement with the observations from the graphic plot of the peak areas vs. the volume of injection in Fig. 5b. Smaller amounts than the equivalent of 0.5 mL injection volume of the calibration gas cannot be detected with the new setup for ethane (~20 nmol in case of C_2H_6, C_2H_4, C_2H_2, CH_4, CO. For helium and hydrogen gas it is apparent that the limit of quantification is reached with 1 mL of gas volume because there is no observable difference between 0.5 mL and 1 mL in the peak area (equals 31 nmol H_2 and 204 nmol He, respectively). The amount of substance was calculated based on the known mol-fraction of the individual gas species i in the calibration standard gas mixture by using the ideal gas equation.

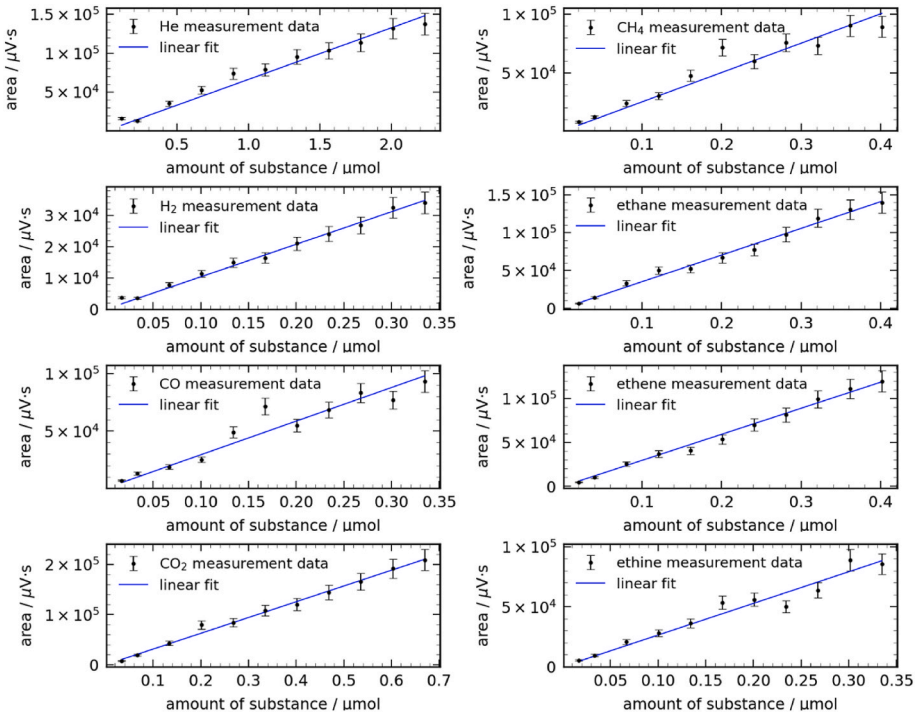

Fig. 7. Measurements and linear fits of the calibration gas were taken using the "gas inlet setup 1″ configuration, which involved injecting defined volumes into a fully evacuated gas pipe.

3.5. Verification of test options for GIS2, test measurements with the simplified test system (STS)

3.5.1. Compact test system with rigid steel container

Firstly, the system was examined using a rigid steel container. In this case, the volume of the sample container V_{cont} does not change with the reduction in pressure. To test the system, the accuracy, precision and reliability of the sample volume determination using the sample loop system was therefore examined. Exact values for volumes, pressures and other parameters used in the following text are listed in Table SI–2 (supporting information).

Under ideal gas conditions and assuming that gas in the evacuated pipe is N_2, equation (2) can be applied when gas is injected from the MFC. In general, the same principle also holds true for injections from a syringe into the GIS1/2 or STS system, in which the gas is introduced completely, similar to the MFC injection. Equation (3) can be used for the amount of substance in V_{cont}. Briefly resumed, n' describes the remaining amount of substance of N_2 in V_{p0}^0 at p_0, n'' the remaining amount of substance of N_2 in V^1 at p_2 and n''' the remaining amount of substance of N_2 in V_s at p_4.

$$p_1 V^0 = (n + n')\, R\, T \tag{2}$$

$$n_{cont.} = \frac{p_1 V_{cont}}{R\, T} \tag{3}$$

By connecting the sample container to the modified gas inlet system (Fig. 4b), both the gas container volume V_{cont} as well as the amount of substance n_{cont} can be calculated (see supporting information, equation SI-1 to SI-3, section 5). However, the use of initial parameters (p_1) is necessary, which are usually unknown in undefined samples. Consequently, the gas switch to the sample loop facilitates the determination of both values, obviating the necessity for the use of initial sample parameters. Equations (4) and (5) can be used to describe the values of volume, pressure and amount of substance. Equations (6) and (7) can then be derived from equations (4) and (5), revealing that the two key values V_{cont} and n_{cont} depend only on parameters that can be easily measured after connecting the gas sample to the gas feed system.

$$p_5\left(V^1 + V_{cont} + V_{SL}\right) = (n_{cont.} + n'' + n''')RT \tag{4}$$

$$p_3\left(V^1 + V_{cont}\right) = (n_{cont.} + n'')RT \tag{5.1}$$

$$n''RT = p_2 V^1 \tag{5.2}$$

$$n'''RT = p_4 V_{SL} \tag{5.3}$$

$$V_{cont.} = \frac{V^1(p_3 - p_5) + V_{SL}(p_4 - p_5)}{p_5 - p_3} \tag{6}$$

$$n_{cont.} = \frac{1}{R\,T}\,\frac{V_{SL}(p_3 p_4 - p_3 p_5) + V^1(p_2 p_3 - p_2 p_5)}{p_5 - p_3} \tag{7}$$

Measurements were taken on this basis and the calculated quantities of amount of substances according to equation (7) were compared with

Table 3
Measurements with the rigid steel container.

test	gas volume applied by MFC	loop system (a)	$V_{cont.}$ (b)	$n_{cont.}$ (c)	$n_{cont.}$ calc. from eq. (7)	deviation
nr.	ml		ml	10^{-4} mol	10^{-4} mol	%
1	3	1	8.729	0.962	0.980	1.9
2	3	1	8.729	1.442	1.483	2.8
3	3	1	8.729	1.218	1.252	2.8
4	3	1	8.729	1.038	1.044	0.5
5	5	1	8.729	1.572	1.603	2.0
6	6	1	8.729	1.848	1.905	3.0
7	8	1	8.729	2.464	2.532	2.8
8	9	1	8.729	2.789	2.886	3.5
9	9	2	8.729	2.771	2.838	2.4
10	12	1	8.729	3.549	3.721	4.9

a) loop system: 1 = sample loop, 2 = gas container; b) taken from Table SI–2; c) calculated from injected volume.

the quantities originally added (Table 3). This revealed excellent agreement, with the majority even falling within the measurement error of the gas container volume itself (Table SI–2).

3.5.2. Compact test system with elastic pouch bag cell

In the second case, the sample volume is not fixed but changes with pressure. For this purpose, a pouch bag cell housing without battery-active components was used (Fig. SI–2, supporting information). Values for volumes, pressures and other parameters are listed in Table 2 and Table SI–2 (supporting information). Assuming ideal gas conditions and knowing that the volume V_1 is not pressure-dependent, equation (2a) as a slightly modified form of equation (2) can be applied when gas is injected from the MFC to the gas sample bag (Fig. 4b). By rewriting, one obtains equations (3a) and (8), where n_{cell} is a function depending on pressure p and volume V_{cell}. The temperature T is assumed to remain constant.

$$p_1 V_{p0}^0 = (n + n')\, R\, T \tag{2a}$$

$$n_{cell}(p, V_{cell}) = \frac{p_1 V_{\mathrm{cell},p1}}{R\, T} \tag{3a}$$

$$V_{\mathrm{cell},p1} = \frac{n\, R\, T + p_0 V_{p0}^0}{p_1} - V_1 \tag{8}$$

The change in volume of the elastic cell with the pressure p has both a linear and an exponential component. For this reason, equation (9) was chosen as the approximation function. This enabled the values to be fitted with a high degree of accuracy (see Fig. SI–3 in the supporting information). Additionally, the fitting values can be used to calculate the actual sample volumes at pressures p_3 and p_5.

$$V_{cell}(p) = a + b{\cdot}p + e^{(c{\cdot}p+d)} \tag{9}$$

The two equations (10) and (11) are used when the sample gas is released into the gas inlet system (STS; Fig. 4a) and when the sample loop is added:

$$p_3 \left(V_{\mathrm{cell},p3} + V^1\right) = (n_c + n'')\, R\, T \tag{10}$$

$$p_5 \left(V_{\mathrm{cell},p5} + V^1 + V_{SL}\right) = (n_c + n'' + n''')\, R\, T \tag{11}$$

The amount of substance n_{cell} can then be calculated using both equations (12) and (13) by rearranging equations (10) and (11).

$$n_{\mathrm{cell}} = \frac{1}{R\, T}\left(p_3 V_{\mathrm{cell},p3} + p_3 V^1 - p_2 V^1\right) \tag{12}$$

$$n_{\mathrm{cell}} = \frac{1}{R\, T}\left(p_5 V_{\mathrm{cell},p5} + p_5 V^1 + p_5 V_{SL} - p_2 V^1 - p_4 V_{SL}\right) \tag{13}$$

To proof the concept, volumes between 3.0 ml and 15.0 ml N_2 were filled into the elastic cell (V^0) from the MFC device and the n_c values were calculated directly by equation (4) and compared with those values, recalculated from equations (12) and (13) (Table 4).

It can be seen that an excellent match of both n_c values is achieved, particularly by using the loop system, both in the sample loop and when using the steel container as a loop. In this case the deviation of the recalculated n_c values from equation (13) is almost less than 10% compared to the initial calculated n_c values, except for one very large gas supply test with 15 ml gas input. The greater deviation in the case of the entered 15 ml results from the pouch cell being so expanded that it reaches the steep rise of the exponential function, resulting in large errors. It should be emphasized that the calculation of the amount of substance according to equations (12) and (13) is based exclusively on the pressure values after the bag has been connected to the gas inlet system.

Both tests (rigid steel container and elastic cell) demonstrate that it is possible to determine the amount of substance contained in a sample cell with a high degree of accuracy over a large range of total gas content in an excellent way. In principle, it is therefore possible to determine the gas content after connecting such sample bags and then immediately perform a GC gas measurement. Using the relative gas composition obtained from the GC measurement and the knowledge of the absolute amount of gas present, the absolute gas contents of the individual gases in the pouch bag cell can then be calculated. While overpressure is possible with fixed sample vessels, it is significantly more critical with flexible cells. In this case, the volume of the sample gas should be small enough that the internal pressure remains below 0.9 bar ($p_3 < 0.9$ bar), so that the equation does not transition into the exponential part.

3.6. Gas adaption to temperature-dependent gas formation setup

To illustrate the wide range of applications, another example is shown, that can be easily realized with the novel gas inlet device. In this

Table 4
Measurements with the elastic sample pouch bag cell.

test	gas volume (a)	loop system (b)	V_{p0}^0 (c)	$V_{\mathrm{cell,\ p1}}$ (d)	n_c (d)	$V_{\mathrm{cell,\ p3}}$ (c)	$V_{\mathrm{cell,\ p5}}$ (c)	n_c calc. from eq. (12)	dev.	n_c calc. from eq. (13)	dev.
nr.	ml		ml	ml	10^{-4} mol	ml	ml	10^{-4} mol	%	10^{-4} mol	%
1	3.0	1	4.01	1.84	0.516	1.26	1.24	0.484	−6.1	0.488	−5.4
2	3.0	1	4.02	1.85	0.523	1.27	1.25	0.480	−8.2	0.485	−7.3
3	3.0	1	4.00	1.90	0.521	1.26	1.24	0.478	−8.2	0.484	−7.2
4	5.0	1	4.02	2.51	1.01	1.39	1.35	0.939	−6.7	0.943	−6.3
5	5.0	1	4.02	2.52	1.01	1.38	1.34	0.905	−10.3	0.911	−9.7
6	5.0	1	4.01	2.48	1.00	1.38	1.34	0.903	−9.7	0.907	−9.3
7	8.0	1	3.99	5.41	2.19	1.68	1.60	2.0	−5.7	2.06	−6.0
8	8.0	1	4.00	5.43	2.21	1.69	1.60	2.12	−4.4	2.11	−4.5
9	8.0	1	4.00	5.42	2.21	1.67	1.59	2.07	−6.4	2.07	−6.4
10	12.0	1	3.99	9.54	3.86	2.08	1.95	3.72	−3.7	3.71	−3.9
11	12.0	1	4.02	9.64	3.90	2.10	1.96	3.80	−2.7	3.78	−3.1
12	12.0	1	3.99	9.48	3.86	2.08	1.94	3.72	−3.6	3.71	−4.0
13	15.0	1	4.01	12.74	5.13	2.26	2.06	4.22	−17.8	4.23	−17.5
14	15.0	1	3.99	12.70	5.11	9.36	2.24	7.31	43.0	4.92	−3.8
15	15.0	1	3.99	12.51	5.10	11.23	2.20	8.17	60.2	4.89	−4.1
16	3	2	3.99	1.77	0.495	1.26	1.20	0.460	−6.9	0.459	−7.1
17	3	2	4.01	1.86	0.518	1.26	1.20	0.468	−9.6	0.478	−7.6
18	5	2	3.99	2.48	0.985	1.38	1.27	0.889	−9.8	0.886	−10.0
19	5	2	3.99	2.48	0.989	1.37	1.26	0.881	−10.9	0.879	−11.1
20	8	2	4.00	5.55	2.23	1.69	1.44	2.09	−6.4	2.05	−8.1
21	12	2	4.00	9.67	3.89	2.10	1.72	3.75	−3.6	3.98	2.4

a) applied by MFC b) loop system: 1 = sample loop, 2 = gas container; c) calculated from fit; d) calculated from injected volume.

case, the GIS1 was used to transfer the sample gas into the GC device without contamination. In the experiment, a solid (25 mg of lithium oxalate) was heated and the gas formed per 100 °C temperature increase was analyzed using GC. The additional setup for gas formation (gas decomposition system) is shown in Fig. 8a.

Since the gas inlet is not designed for high temperatures of several hundred degrees, the gas formed was cooled to room temperature and introduced at RT. Note that cooling can cause water vapor to condense. However, cooling does not affect the compounds CO and CO_2, as neither oxygen nor catalysts are present to cause them to convert into each other. The gas decomposition system was then connected directly to GIS1 using a quick coupling, and the gas was completely evacuated after each analysis (the entire gas chamber from the furnace to the GC) so that the newly formed gas mixture could always be observed. With this setup, it was possible to measure and quantify the respective amounts of CO and CO_2 formed in different temperature ranges after cooling to room temperature (Fig. 8b). Starting at 400 °C, both compounds form in almost equal amounts (moles), and between 500 and 550 °C, a pronounced formation of CO and CO_2 can be observed (decomposition of 25 mg lithium oxalate). The main benefit is that the gas can be completely evacuated after each measurement, so that existing gas does not cause interferring signals, when the temperature is raised again. This makes it possible to actually evaluate temperature-dependent processes. Additionally, the GC setup enables a separation of the gas species which can not be achieved in case of other analytical tools, like DEMS or IR analysis.

3.7. Gas adaption to battery cells

Main drawbacks remain for the transfer of pouch-bag gas to the GIS1 and GIS2 when a syringe is used for the gas transfer via septum injection (Fig. 9a). Fortunately, the design of the novel setup allows the simple adaptation of further connection options, such as a direct connection to a battery cell or an adaptation to sample gas from a gas bomb via Swagelok female quick connect adapters. A modified, more sophisticated and restricted approach is presented by Wang et al., where a catheter like tube which was sealed by a rubber cap was inserted into the pouch bag cell during sealing [29].

Although the introduction of a newly developed pouch cell including gas adaption, including complete validation, goes far beyond the scope of this manuscript, it is briefly shown how such an adaptation can be achieved. For instance, a stainless steel line can be connected directly to the cell during cell construction. Since no large attachments are possible during the sealing process, the valves are then attached to the initially closed stainless steel pipe in a two-step process immediately after cell construction (Fig. 9b), and the cell is again set to the desired final vacuum.

The main advantages of the setup are (1) the adapter is already permanently attached onto the pouch-bag foil at the beginning of cell assembly, which eliminates the need for subsequent piercing, (2) the cell gases can be introduced directly into the GC without dilution and syringe handling, and (3) since the connection is permanently sealed, cells can be cycled and measured in the same way as cells without adapters.

A direct comparison of cell cycling with and without adapter is shown in Fig. SI–4 in the supporting information for the cell formation period. This reveals unchanged cycling behavior in the case of cells with adapter, so that no significant deterioration can be assumed. A slight improvement in case of using the gas adapter during the first cycle (increased energy efficiency due to reduced cell potentials) might arise from the enlarged evacuated line in case of the additional adapter which causes a lower internal pressure of the pouch cell.

It should be noted that, as an elastic cell, the pouch bag cell has a volume that is unfortunately not constant over a pressure range. However, the setup allows the determination of this volume and to calculate the original total amount of gas in the cell. This makes it possible to calculate absolute quantities of individual gases formed in the cell in the course of cycling, and in this way to accurately track gas formation under real conditions.

4. Conclusions

In this article, we present a versatile setup that can perform quantitative gas measurements with a small sample volume of 0.5 to 15 mL. Even samples under low and reduced pressure can be processed. The advantages of this setup extend far beyond the battery sector. Any type of sample container can be analyzed easily and reliably, and reliable statements about the gas composition can be made. Depending on the gas chromatography (GC) equipment used (e.g., detectors, gas system), the corresponding gases can be easily determined. This greatly simplifies the widespread use of error-prone injection methods with syringes and/or complex adapter systems and eliminates the need for multiple measurements to determine gas volume and content. Sample measurements on calibration gas mixtures, nitrogen, and lithium oxalate demonstrate the approach's fundamental suitability. The newly developed cell adapter enables in situ measurement of battery gas because the cells can operate without contamination after measurement and maintain the desired pressure. The pouch cell connection allows for measurement of cells under defined vacuum conditions. Automating the system can further simplify the technology. For this reason, the presented method is expected to be useful in various chemical and biochemical applications, offering significant benefits.

CRediT authorship contribution statement

Andreas Hofmann: Writing – review & editing, Writing – original draft, Visualization, Validation, Resources, Methodology, Investigation, Funding acquisition, Formal analysis, Conceptualization. **Ingo Reuter:** Writing – review & editing, Investigation, Formal analysis. **Freya Müller:** Writing – review & editing, Visualization, Investigation, Formal analysis, Data curation. **Anna Smith:** Writing – review & editing, Supervision, Resources, Conceptualization.

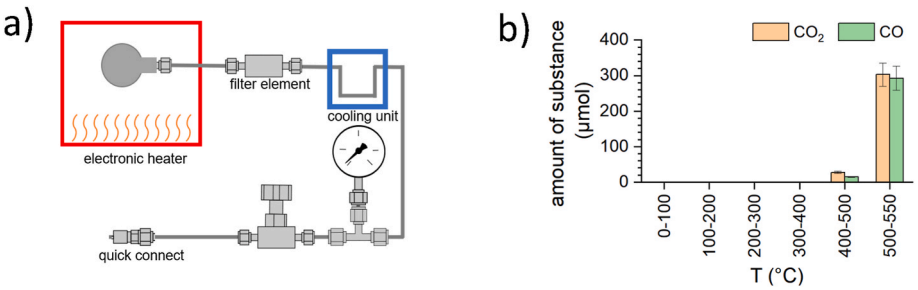

Fig. 8. a: Setup for detecting temperature-controlled decomposition reactions.b: Example of gas generation from lithium oxalate at selected temperatures. Measurements were taken after each 100 °C temperature increase.

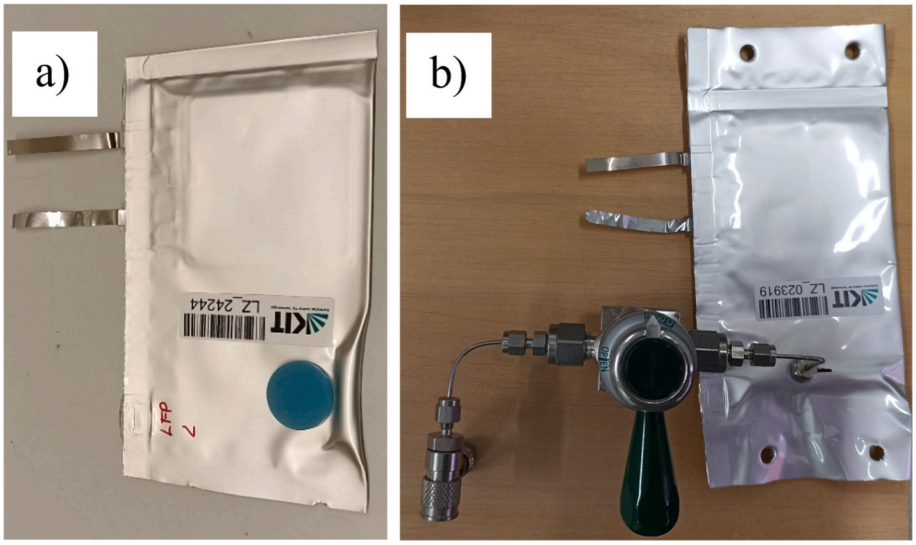

Fig. 9. a: A pouch bag cell with a septum for syringe extraction is shown. b: Image of a pouch-bag sample bag with a Swagelok quick connect adapter for contamination-free gas extraction.

Raw data and supporting information

Supporting information is provided as separate file.

Raw data of the pressure and volume are available at Zenodo.org (https://10.5281/zenodo.18607963).

Declaration of competing interest

The authors declare the following financial interests/personal relationships which may be considered as potential competing interests: Andreas Hofmann reports article publishing charges was provided by German Research Foundation. Andreas Hofmann reports financial support was provided by German Research Foundation. Andreas Hofmann has patent pending to Karlsruher Institut für Technologie. Anna Smith has patent pending to Karlsruher Institut für Technologie. Ingo Reuter has patent pending to Karlsruher Institut für Technologie. Freya Mueller has patent pending to Karlsruher Institut für Technologie.

Acknowledgements

The cell assembling was done at KIT Battery Technology Center (KIT-BATEC). This work contributes to the research performed at CELEST (Center for Electrochemical Energy Storage Ulm-Karlsruhe) and was funded by the German Research Foundation (DFG) under Project ID 390874152 (POLiS Cluster of Excellence).

Appendix A. Supplementary data

Supplementary data to this article can be found online at https://doi.org/10.1016/j.aca.2026.345217.

Data availability

Data will be provided at Zenodo.org, we will include the link in the proof version.

References

[1] P. Liu, L. Yang, B. Xiao, H. Wang, L. Li, S. Ye, Y. Li, X. Ren, X. Ouyang, J. Hu, F. Pan, Q. Zhang, J. Liu, Revealing Lithium battery gas generation for safer practical applications, Adv. Funct. Mater. 32 (2022) 2208586–2208608, https://doi.org/10.1002/adfm.202208586.

[2] R. Fong, M.C. Reid, R.S. McMillan, J.R. Dahn, In situ Study of electrolyte reactions in secondary lithium cells, J. Electrochem. Soc. 134 (1987) 516–519, https://doi.org/10.1149/1.2100501.

[3] Y.P. Stenzel, F. Horsthemke, M. Winter, S. Nowak, Chromatographic techniques in the research area of lithium ion batteries: current state-of-the-art, Separations 6 (2019) 26–72, https://doi.org/10.3390/separations6020026.

[4] B. Rowden, N. Garcia-Araez, A review of gas evolution in lithium ion batteries, Energy Rep. 6 (2020) 10–18, https://doi.org/10.1016/j.egyr.2020.02.022.

[5] E.J.K. Nilsson, A. Ahlberg Tidblad, Gas emissions from lithium-ion batteries: a review of experimental results and methodologies, Batteries 10 (2024) 443–478, https://doi.org/10.3390/batteries10120443.

[6] I. Adanouj, A. Kriston, V. Ruiz, A. Pfrang, Identification and quantification of decomposition mechanisms in lithium-ion batteries; input to heat flow simulation for modeling thermal runaway, J. Vis. Exp. (2022) e62376, https://doi.org/10.3791/62376.

[7] G. Gachot, S. Grugeon, I. Jimenez-Gordon, G.G. Eshetu, S. Boyanov, A. Lecocq, G. Marlair, S. Pilard, S. Laruelle, Gas chromatography/Fourier transform infrared/mass spectrometry coupling: a tool for Li-ion battery safety field investigation, Anal. Methods 6 (2014) 6120–6124, https://doi.org/10.1039/c4ay00054d.

[8] C. Mao, R.E. Ruther, L. Geng, Z. Li, D.N. Leonard, H.M. Meyer 3rd, R.L. Sacci, D. L. Wood 3rd, Evaluation of gas Formation and consumption driven by crossover effect in high-voltage lithium-ion batteries with Ni-Rich NMC cathodes, ACS Appl. Mater. Interfaces 11 (2019) 43235–43243, https://doi.org/10.1021/acsami.9b15916.

[9] F. Diaz, Y. Wang, R. Weyhe, B. Friedrich, Gas generation measurement and evaluation during mechanical processing and thermal treatment of spent Li-ion batteries, Waste Manag. 84 (2019) 102–111, https://doi.org/10.1016/j.wasman.2018.11.029.

[10] Y. Fernandes, A. Bry, S. de Persis, Identification and quantification of gases emitted during abuse tests by overcharge of a commercial Li-ion battery, J. Power Sources 389 (2018) 106–119, https://doi.org/10.1016/j.jpowsour.2018.03.034.

[11] F. Larsson, P. Andersson, P. Blomqvist, A. Lorén, B.-E. Mellander, Characteristics of lithium-ion batteries during fire tests, J. Power Sources 271 (2014) 414–420, https://doi.org/10.1016/j.jpowsour.2014.08.027.

[12] M. Börner, A. Friesen, M. Grützke, Y.P. Stenzel, G. Brunklaus, J. Haetge, S. Nowak, F.M. Schappacher, M. Winter, Correlation of aging and thermal stability of commercial 18650-type lithium ion batteries, J. Power Sources 342 (2017) 382–392, https://doi.org/10.1016/j.jpowsour.2016.12.041.

[13] R. Mogi, M. Inaba, Y. Iriyama, T. Abe, Z. Ogumi, Study of the decomposition of propylene carbonate on lithium metal surface by Pyrolysis−Gas chromatography−mass spectroscopy, Langmuir 19 (2003) 814–821, https://doi.org/10.1021/la026299b.

[14] Z. Ogumi, A. Sano, M. Inaba, T. Abe, Pyrolysis/gas chromatography/mass spectroscopy analysis of the surface film formed on graphite negative electrode, J. Power Sources 97 (2001) 156–158, https://doi.org/10.1016/S0378-7753(01)00529-8.

[15] P. Wang, L. Chen, Y. Shen, Recycling spent ternary lithium-ion batteries for modification of dolomite used in catalytic biomass pyrolysis - a preliminary study by thermogravimetric and pyrolysis-gas chromatography/mass spectrometry analysis, Bioresour. Technol. 337 (2021) 125476–125482, https://doi.org/10.1016/j.biortech.2021.125476.

[16] W. Xu, V.V. Viswanathan, D. Wang, S.A. Towne, J. Xiao, Z. Nie, D. Hu, J.-G. Zhang, Investigation on the charging process of Li2O2-based air electrodes in Li-O2 batteries with organic carbonate electrolytes, J. Power Sources 196 (2011) 3894–3899, https://doi.org/10.1016/j.jpowsour.2010.12.065.

[17] M. Metzger, C. Marino, J. Sicklinger, D. Haering, H.A. Gasteiger, Anodic oxidation of conductive carbon and ethylene carbonate in high-voltage Li-Ion batteries quantified by On-Line electrochemical mass spectrometry, J. Electrochem. Soc. 162 (2015) A1123–A1134, https://doi.org/10.1149/2.0951506jes.

[18] B.B. Berkes, A. Jozwiuk, H. Sommer, T. Brezesinski, J. Janek, Simultaneous acquisition of differential electrochemical mass spectrometry and infrared spectroscopy data for in situ characterization of gas evolution reactions in lithium-ion batteries, Electrochem. Commun. 60 (2015) 64–69, https://doi.org/10.1016/j.elecom.2015.08.002.

[19] B.B. Berkes, A. Jozwiuk, M. Vracar, H. Sommer, T. Brezesinski, J. Janek, Online continuous flow differential electrochemical mass spectrometry with a realistic battery setup for High-Precision, long-term cycling tests, Anal. Chem. 87 (2015) 5878–5883, https://doi.org/10.1021/acs.analchem.5b01237.

[20] J. Geisler, L. Pfeiffer, G.A. Ferrero, P. Axmann, P. Adelhelm, Setup design and data evaluation for DEMS in sodium ion batteries, demonstrated on a Mn-Rich cathode material, Batter. Supercaps 7 (2024) e202400006, https://doi.org/10.1002/batt.202400006.

[21] L. Reuter, J.L.S. Dickmanns, B. Strehle, L. Hartmann, F. Maglia, R. Jung, B. Suthar, H.A. Gasteiger, Methods–Temperature-Dependent gassing analysis by On-Line electrochemical mass spectrometry of lithium-ion battery cells with commercial electrolytes, J. Electrochem. Soc. 171 (2024) 50551–50576, https://doi.org/10.1149/1945-7111/ad4311.

[22] H. Zhang, J. Chen, Y. Hong, X. Wu, X. Huang, P. Dai, H. Luo, B. Zhang, Y. Qiao, S. G. Sun, Titration Mass Spectroscopy (TMS): a quantitative analytical technology for rechargeable batteries, Nano Lett. 22 (2022) 9972–9981, https://doi.org/10.1021/acs.nanolett.2c03535.

[23] M. Metzger, H.A. Gasteiger, Diagnosing battery degradation via gas analysis, Energy Environ. Mater. 5 (2022) 688–692, https://doi.org/10.1002/eem2.12326.

[24] T. Zheng, M. Muneeswara, H. Bao, J. Huang, L. Zhang, D.S. Hall, S.T. Boles, W. Jin, Gas evolution in Li-Ion rechargeable batteries: a review on operando sensing technologies, gassing mechanisms, and emerging trends, Chemelectrochem 11 (2024) e202400065, https://doi.org/10.1002/celc.202400065.

[25] H. Li, S. Guo, H. Zhou, In-situ/operando characterization techniques in lithium-ion batteries and beyond, J. Energy Chem. 59 (2021) 191–211, https://doi.org/10.1016/j.jechem.2020.11.020.

[26] S. Kim, H.-S. Kim, B. Kim, Y.-J. Kim, J.-W. Jung, W.-H. Ryu, In situ gas analysis by differential electrochemical mass spectrometry for advanced rechargeable batteries: a review, Adv. Energy Mater. 13 (2023) 2301983–2302015, https://doi.org/10.1002/aenm.202301983.

[27] S. Lyu, N. Li, L. Sun, S. Jiao, H. Chen, W.-L. Song, Rapid operando gas monitor for commercial lithium ion batteries: gas evolution and relation with electrode materials, J. Energy Chem. 72 (2022) 14–25, https://doi.org/10.1016/j.jechem.2022.04.010.

[28] J. Liu, P. Bian, J. Li, W. Ji, H. Hao, A. Yu, Gassing behavior of lithium titanate based lithium ion batteries with different types of electrolytes, J. Power Sources 286 (2015) 380–387, https://doi.org/10.1016/j.jpowsour.2015.03.172.

[29] S. Wang, J. Liu, K. Rafiz, Y. Jin, Y. Li, Y.S. Lin, An On-Line transient Study on gassing mechanism of lithium titanate batteries, J. Electrochem. Soc. 166 (2019) A4150–A4157, https://doi.org/10.1149/2.0631916jes.

[30] C.P. Aiken, J. Xia, D.Y. Wang, D.A. Stevens, S. Trussler, J.R. Dahn, An Apparatus for the Study of in situ gas evolution in Li-Ion pouch cells, J. Electrochem. Soc. 161 (2014) A1548–A1554, https://doi.org/10.1149/2.0151410jes.

[31] M. Leißing, F. Horsthemke, S. Wiemers-Meyer, M. Winter, P. Niehoff, S. Nowak, The impact of the c-rate on gassing during Formation of NMC622 II graphite lithium-ion battery cells, Batter. Supercaps 4 (2021) 1344–1350, https://doi.org/10.1002/batt.202100056.

[32] E.R. Logan, A. Eldesoky, E. Eastwood, H. Hebecker, C.P. Aiken, M. Metzger, J. R. Dahn, The use of LiFSI and LiTFSI in LiFePO4/Graphite pouch cells to improve high-temperature lifetime, J. Electrochem. Soc. 169 (2022) 40560–40578, https://doi.org/10.1149/1945-7111/ac67f9.

[33] M.S. Milien, J. Hoffmann, M. Payne, B.L. Lucht, Effect of electrolyte additives on Li4Ti5O12 cycling performance and gas evolution, J. Electrochem. Soc. 165 (2018) A3925–A3931, https://doi.org/10.1149/2.0741816jes.

[34] D.J. Xiong, L.D. Ellis, K.J. Nelson, T. Hynes, R. Petibon, J.R. Dahn, Rapid impedance growth and gas production at the Li-Ion cell positive electrode in the absence of a negative electrode, J. Electrochem. Soc. 163 (2016) A3069–A3077, https://doi.org/10.1149/2.1031614jes.

[35] K.H. Lee, E.H. Song, J.Y. Lee, B.H. Jung, H.S. Lim, Mechanism of gas build-up in a Li-ion cell at elevated temperature, J. Power Sources 132 (2004) 201–205, https://doi.org/10.1016/j.jpowsour.2004.01.042.

[36] H. Zhang, Y. Peng, K. Zhang, S. Tang, Y. Wei, J. Liang, Y. Jin, Y. Yang, Protocol for quantifying all electrolyte compositions in aged lithium-ion batteries, Batter. Supercaps 7 (2024) e202400341, https://doi.org/10.1002/batt.202400341.

[37] J.-Y. Eom, I.-H. Jung, J.-H. Lee, Effects of vinylene carbonate on high temperature storage of high voltage Li-ion batteries, J. Power Sources 196 (2011) 9810–9814, https://doi.org/10.1016/j.jpowsour.2011.06.095.

[38] C.R. Fell, L. Sun, P.B. Hallac, B. Metz, B. Sisk, Investigation of the gas generation in lithium titanate anode based lithium ion batteries, J. Electrochem. Soc. 162 (2015) A1916–A1920, https://doi.org/10.1149/2.1091509jes.

[39] Y. Kim, Investigation of the gas evolution in lithium ion batteries: effect of free lithium compounds in cathode materials, J. Solid State Electrochem. 17 (2013) 1961–1965, https://doi.org/10.1007/s10008-013-2050-2.

[40] K.W. Leitner, H. Wolf, A. Garsuch, F. Chesneau, M. Schulz-Dobrick, Electroactive separator for high voltage graphite/$LiNi_{0.5}Mn_{1.5}O_4$ lithium ion batteries, J. Power Sources 244 (2013) 548–551, https://doi.org/10.1016/j.jpowsour.2013.01.187.

[41] J. Sun, J. Li, T. Zhou, K. Yang, S. Wei, N. Tang, N. Dang, H. Li, X. Qiu, L. Chen, Toxicity, a serious concern of thermal runaway from commercial Li-ion battery, Nano Energy 27 (2016) 313–319, https://doi.org/10.1016/j.nanoen.2016.06.031.

[42] B. Surampudi, K. Jones, B. Shuvodeep Bhattacharyya, A comparative Study of lithium-ion cathode chemistry correlations with emissions initiated by nail penetration abuse in the presence of an immersive coolant, SAE Tech. Pap. 5 (2023) 392–403, https://doi.org/10.4271/2022-01-0707.

[43] K. Zou, S. Lu, X. Chen, E. Gao, Y. Cao, Y. Bi, Thermal and gas characteristics of large-format LiNi0.8Co0.1Mn0.1O2 pouch power cell during thermal runaway, J. Energy Storage 39 (2021) 102609–102617, https://doi.org/10.1016/j.est.2021.102609.

[44] S. Ciorba, M. Marracci, C. Antonetti, M. Martinelli, G. Caposciutti, B. Tellini, A. M. Raspolli Galletti, Experimental analysis of overcharged Li-polymer batteries, Case Stud. Chem. Environ. Eng. 2 (2020), https://doi.org/10.1016/j.cscee.2020.100012.

[45] K. Homlamai, N. Anansuksawat, T. Sangsanit, S. Prempluem, K. Santisuk, W. Tejangkura, M. Sawangphruk, Gas evolution analyses of Ni-rich Li-ion and Li-metal batteries at cylindrical jelly-roll configurations, J. Power Sources 617 (2024) 235150–235159, https://doi.org/10.1016/j.jpowsour.2024.235150.

[46] M. Yang, M. Rong, Y. Ye, A. Yang, J. Chu, H. Yuan, X. Wang, Comprehensive analysis of gas production for commercial LiFePO4 batteries during overcharge-thermal runaway, J. Energy Storage 72 (2023) 108323–108332, https://doi.org/10.1016/j.est.2023.108323.

[47] D.P. Abraham, E.P. Roth, R. Kostecki, K. McCarthy, S. MacLaren, D.H. Doughty, Diagnostic examination of thermally abused high-power lithium-ion cells, J. Power Sources 161 (2006) 648–657, https://doi.org/10.1016/j.jpowsour.2006.04.088.

[48] J.-P. Brinkmann, N. Ehteshami-Flammer, M. Luo, M. Leißing, S. Röser, S. Nowak, Y. Yang, M. Winter, J. Li, Compatibility of various electrolytes with cation disordered Rocksalt cathodes in lithium ion batteries, ACS Appl. Energy Mater. 4 (2021) 10909–10920, https://doi.org/10.1021/acsaem.1c01879.

[49] W. Kong, H. Li, X. Huang, L. Chen, Gas evolution behaviors for several cathode materials in lithium-ion batteries, J. Power Sources 142 (2005) 285–291, https://doi.org/10.1016/j.jpowsour.2004.10.008.

[50] M. Leißing, C. Peschel, F. Horsthemke, S. Wiemers-Meyer, M. Winter, S. Nowak, The origin of gaseous decomposition products formed during SEI Formation analyzed by isotope labeling in lithium-ion battery electrolytes, Batter. Supercaps 4 (2021) 1731–1738, https://doi.org/10.1002/batt.202100208.

[51] M. Leißing, M. Winter, S. Wiemers-Meyer, S. Nowak, A method for quantitative analysis of gases evolving during formation applied on LiNi0.6Mn0.2Co0.2O2 mid r:mid R: natural graphite lithium ion battery cells using gas chromatography - barrier discharge ionization detector, J. Chromatogr. A 1622 (2020) 461122–461128, https://doi.org/10.1016/j.chroma.2020.461122.

[52] M. Onuki, S. Kinoshita, Y. Sakata, M. Yanagidate, Y. Otake, M. Ue, M. Deguchi, Identification of the source of evolved gas in Li-Ion batteries using [sup 13]C-labeled solvents, J. Electrochem. Soc. 155 (2008) A794–A797, https://doi.org/10.1149/1.2969947.

[53] H. Schneider, T. Weiß, C. Scordilis-Kelley, J. Maeyer, K. Leitner, H.-J. Peng, R. Schmidt, J. Tomforde, Electrolyte decomposition and gas evolution in a lithium-sulfur cell upon long-term cycling, Electrochim. Acta 243 (2017) 26–32, https://doi.org/10.1016/j.electacta.2017.05.034.

[54] J.-S. Shin, C.-H. Han, U.-H. Jung, S.-I. Lee, H.-J. Kim, K. Kim, Effect of Li2CO3 additive on gas generation in lithium-ion batteries, J. Power Sources 109 (2002) 47–52, https://doi.org/10.1016/s0378-7753(02)00039-3.

[55] L. Bai, J. Smuts, P. Walsh, H. Fan, Z. Hildenbrand, D. Wong, D. Wetz, K.A. Schug, Permanent gas analysis using gas chromatography with vacuum ultraviolet detection, J. Chromatogr. A 1388 (2015) 244–250, https://doi.org/10.1016/j.chroma.2015.02.007.

[56] K. Kumai, H. Miyashiro, Y. Kobayashi, K. Takei, R. Ishikawa, Gas generation mechanism due to electrolyte decomposition in commercial lithium-ion cell, J. Power Sources 81–82 (1999) 715–719, https://doi.org/10.1016/S0378-7753(98)00234-1.

[57] C. Fang, J. Li, M. Zhang, Y. Zhang, F. Yang, J.Z. Lee, M.H. Lee, J. Alvarado, M. A. Schroeder, Y. Yang, B. Lu, N. Williams, M. Ceja, L. Yang, M. Cai, J. Gu, K. Xu, X. Wang, Y.S. Meng, Quantifying inactive lithium in lithium metal batteries, Nature 572 (2019) 511–515, https://doi.org/10.1038/s41586-019-1481-z.

[58] X. Zhang, S. Weng, G. Yang, Y. Li, H. Li, D. Su, L. Gu, Z. Wang, X. Wang, L. Chen, Interplay between solid-electrolyte interphase and (in)active LixSi in silicon anode, Cell Rep. Phys. Sci. 2 (2021) 100668–100679, https://doi.org/10.1016/j.xcrp.2021.100668.

[59] T. Ohsaki, T. Kishi, T. Kuboki, N. Takami, N. Shimura, Y. Sato, M. Sekino, A. Satoh, Overcharge reaction of lithium-ion batteries, J. Power Sources 146 (2005) 97–100, https://doi.org/10.1016/j.jpowsour.2005.03.105.

[60] A.W. Golubkov, S. Scheikl, R. Planteu, G. Voitic, H. Wiltsche, C. Stangl, G. Fauler, A. Thaler, V. Hacker, Thermal runaway of commercial 18650 Li-ion batteries with LFP and NCA cathodes – impact of state of charge and overcharge, RSC Adv. 5 (2015) 57171–57186, https://doi.org/10.1039/c5ra05897j.

[61] L.D. Ellis, J.P. Allen, L.M. Thompson, J.E. Harlow, W.J. Stone, I.G. Hill, J.R. Dahn, Quantifying, understanding and evaluating the effects of gas consumption in lithium-ion cells, J. Electrochem. Soc. 164 (2017) A3518–A3528, https://doi.org/10.1149/2.0191714jes.

[62] R. Petibon, L.M. Rotermund, J.R. Dahn, Evaluation of phenyl carbonates as electrolyte additives in lithium-ion batteries, J. Power Sources 287 (2015) 184–195, https://doi.org/10.1016/j.jpowsour.2015.04.012.

[63] J. Self, C.P. Aiken, R. Petibon, J.R. Dahn, Survey of gas expansion in Li-Ion NMC pouch cells, J. Electrochem. Soc. 162 (2015) A796–A802, https://doi.org/10.1149/2.0081506jes.

[64] D.J. Xiong, T. Hynes, L.D. Ellis, J.R. Dahn, Effects of surface coating on gas evolution and impedance growth at Li[NixMnyCo1-x-y]O2Positive electrodes in Li-Ion cells, J. Electrochem. Soc. 164 (2017) A3174–A3181, https://doi.org/10.1149/2.0991713jes.

[65] M. Grützke, S. Krüger, V. Kraft, B. Vortmann, S. Rothermel, M. Winter, S. Nowak, Investigation of the storage behavior of shredded lithium-ion batteries from electric vehicles for recycling purposes, ChemSusChem 8 (2015) 3433–3438, https://doi.org/10.1002/cssc.201500920.

[66] F. Horsthemke, M. Leißing, V. Winkler, A. Friesen, L. Ibing, M. Winter, S. Nowak, Development of a lithium ion cell enabling in situ analyses of the electrolyte using gas chromatographic techniques, Electrochim. Acta 338 (2020) 135894–135901, https://doi.org/10.1016/j.electacta.2020.135894.

[67] C. Peschel, F. Horsthemke, M. Leißing, S. Wiemers-Meyer, J. Henschel, M. Winter, S. Nowak, Analysis of Carbonate decomposition during solid electrolyte interphase Formation in isotope-labeled lithium ion battery electrolytes: extending the knowledge about electrolyte soluble species, Batter. Supercaps 3 (2020) 1183–1192, https://doi.org/10.1002/batt.202000170.

[68] H. Ota, A. Kominato, W.-J. Chun, E. Yasukawa, S. Kasuya, Effect of cyclic phosphate additive in non-flammable electrolyte, J. Power Sources 119–121 (2003) 393–398, https://doi.org/10.1016/s0378-7753(03)00259-3.

[69] H. Ota, T. Sato, H. Suzuki, T. Usami, TPD-GC/MS analysis of the solid electrolyte interface (SEI) on a graphite anode in the propylene carbonate/ethylene sulfite electrolyte system for lithium batteries, J. Power Sources 97 (2001) 107–113, https://doi.org/10.1016/S0378-7753(01)00738-8.

[70] L. Geng, D.L. Wood, S.A. Lewis, R.M. Connatser, M. Li, C.J. Jafta, I. Belharouak, High accuracy in-situ direct gas analysis of Li-ion batteries, J. Power Sources 466 (2020) 228211–228219, https://doi.org/10.1016/j.jpowsour.2020.228211.

[71] G. Gachot, P. Ribière, D. Mathiron, S. Grugeon, M. Armand, J.-B. Leriche, S. Pilard, S. Laruelle, Gas Chromatography/Mass spectrometry as a suitable tool for the Li-Ion battery electrolyte degradation mechanisms Study, Anal. Chem. 83 (2011) 478–485, https://doi.org/10.1021/ac101948u.

[72] H. Zhang, X. Wu, Z. Li, Y. Zou, J. Wang, X. Yu, J. Chen, J. Xue, B. Zhang, J.-H. Tian, Y.-h. Hong, Y. Qiao, S.-G. Sun, Full-Dimensional analysis of gaseous products within Li-Ion batteries by On-Line GC-BID/MS, Adv. Energy Mater. 14 (2024) 2400397–2400406, https://doi.org/10.1002/aenm.202400397.

[73] A. Smith, P. Stüble, L. Leuthner, A. Hofmann, F. Jeschull, L. Mereacre, Potential and limitations of research battery cell types for electrochemical data acquisition, Batter. Supercaps 6 (2023) e202300080, https://doi.org/10.1002/batt.202300080.